"A modeling study of the long-term mineral trapping in deep saline marine sand aquifers"

P. Aagaard, Pham, V.T.H, and Hellevang, H,
Dep of Geosciences, University of Oslo, PO Box 1047 Blindern, 0316 Oslo, Norway

GSA 14.12.2009

CO_2-Water-Rock Interactions in Geologic Storage

- How well are we presently able to simulate CO_2 fate and transport in reservoir filling?
- Uncertainties in multiphase reactive transport:
  - Geological model – geometry, heterogeneity
  - Two phase flow – rel perm, capillary pressure
  - Phase behavior – solubility, comp.effects
  - Water rock interactions – thermodynamics/kinetics
- Focus here: How well do we represent these geochemical reactions in our simulations?

How well do we represent these geochemical reactions in our simulations?

- Kinetics of water rock interactions
- Substrate for nucleation and growth
- Mineralogical compositions

Utsira case w/parameter sensitivity

Why is dawsonite often absent in CO_2 charged reservoirs?

- Dawsonite is less abundant in natural analogues (except where the aquifers are highly alkaline or where large concentrations of Na-feldspar have been locally replaced)

- The answer on the differences between observed and simulated dawsonite growth may be found in the way the numerical codes solve for the thermodynamic and kinetic stability.

- the classical way of simulating mineral growth is by using a single-affinity-term TST-derived rate law (Transition State Theory)

- fails to capture the differences in mechanisms of dissolution and growth

Commonly used TST derived rate expressions used both for dissolution and precipitation

$$r = kS\prod_i \mathbf{a}_i^m \exp\left(-\frac{Ea}{RT}\right) f(\Delta G)$$

$$f(\Delta G) = 1 - \exp\left(\frac{\Delta G}{\sigma RT}\right)$$

$$S = \beta Mn$$

where β is the Brunauer-Emmet-Teller (BET) specific surface area, M is the molar weight and n is the number of moles of the mineral,

whereas the reactive surface area for precipitation of new minerals often is set equal to 1% of the total sediment surface area. This number, representing a fraction of the total surface area, has no direct physical meaning but is in the range of what have been used in other numerical studies on mineral formation during CO_2 storage (e.g., Gaus et al., 2005; Johnson et al., 2004)

Precipitation rate considerations including a critical super-saturation

Recent work on carbonate reactivity strongly suggest that precipitation rates may be orders of magnitude lower than those estimated from corresponding dissolution rates by TST (e.g., compare Pokrovsky et al., 2009; Saldi et al., 2009)

Introduced a critical super-saturation that corresponds to the nucleation barrier at low temperatures and applied a second order affinity dependence as seen for spiral growth (Hellevang et al., 2009)

Reactive surface area for growth of new product minerals, expressed through an initial area for nucleation and growth.

Dawsonite precipitation

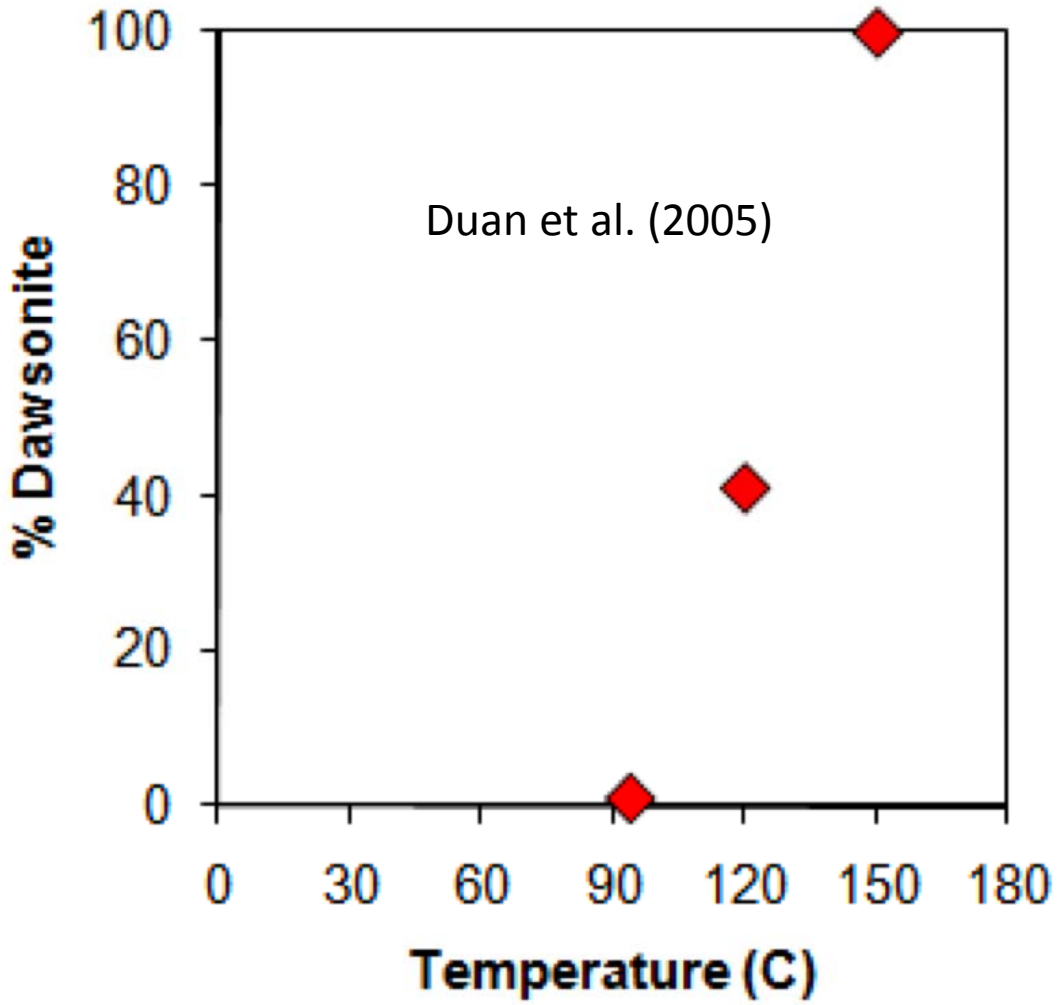

Even at very high supersatutations dawsonite rapidly stops precipitating in measurable amounts as soon as the temperature drops below 70-90°C (Duan et al., 2005)

Magnesite precipitation

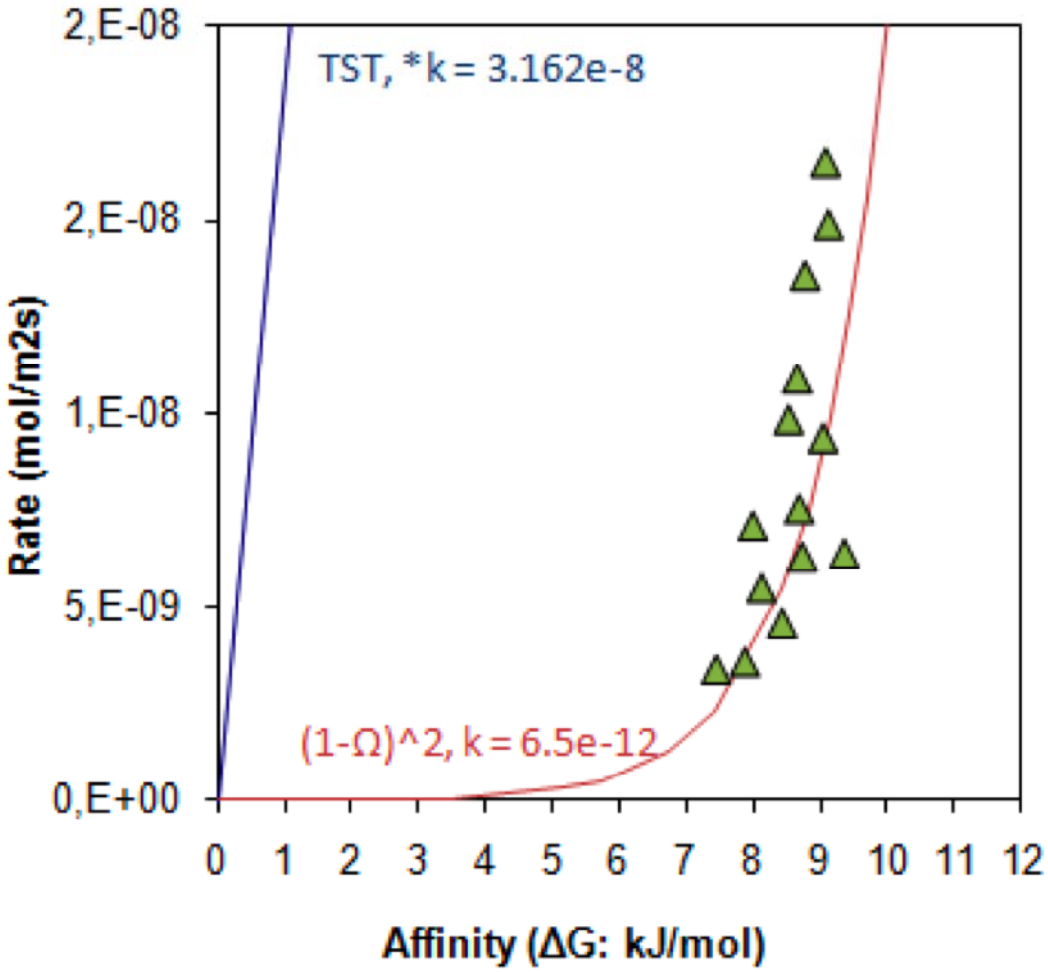

The difference in calculated precipitation rates of magnesite

1) using the traditional TST-derived equation based on the far-from-equilibrium dissolution rate data from Pokrovsky et al. (2009),and
2) calculation according to critical supersaturation from the experimental data by Saldi et al. (2009)

Precipitation rate constants smaller and including a critical super-saturation

$$r = \begin{cases} k_d S_d \mathbf{a}_i^{m_d} \exp\left(-\frac{Ea_d}{RT}\right)\{1-\Omega\} & if \quad \Omega < 1 \quad \text{undersaturation condition} \\ 0 & if \quad 1 \le \Omega \le \Omega_c \quad \text{supersat lower than critical} \\ \tau \cdot k_p S_p \mathbf{a}_i^{m_p} \exp\left(-\frac{Ea_P}{RT}\right)\{\Omega_c - \Omega\}^{\omega} & if \quad \Omega_c < \Omega \quad \text{supersaturation over critical} \end{cases}$$

superscript ω is a coefficient that depends on the growth mechanism, where $\omega = 1$ results from transport or adsorption controlled growth and $\omega = 2$ from spiral growth (Nielsen, 1983), and τ is -1 or 1 for $\omega = 2$ or 1 respectively.

$$S_p = \alpha + \beta Mn \qquad S_d = \beta Mn$$

where α is the reactive surface area for growth for the precipitating mineral.

Utsira case revisited

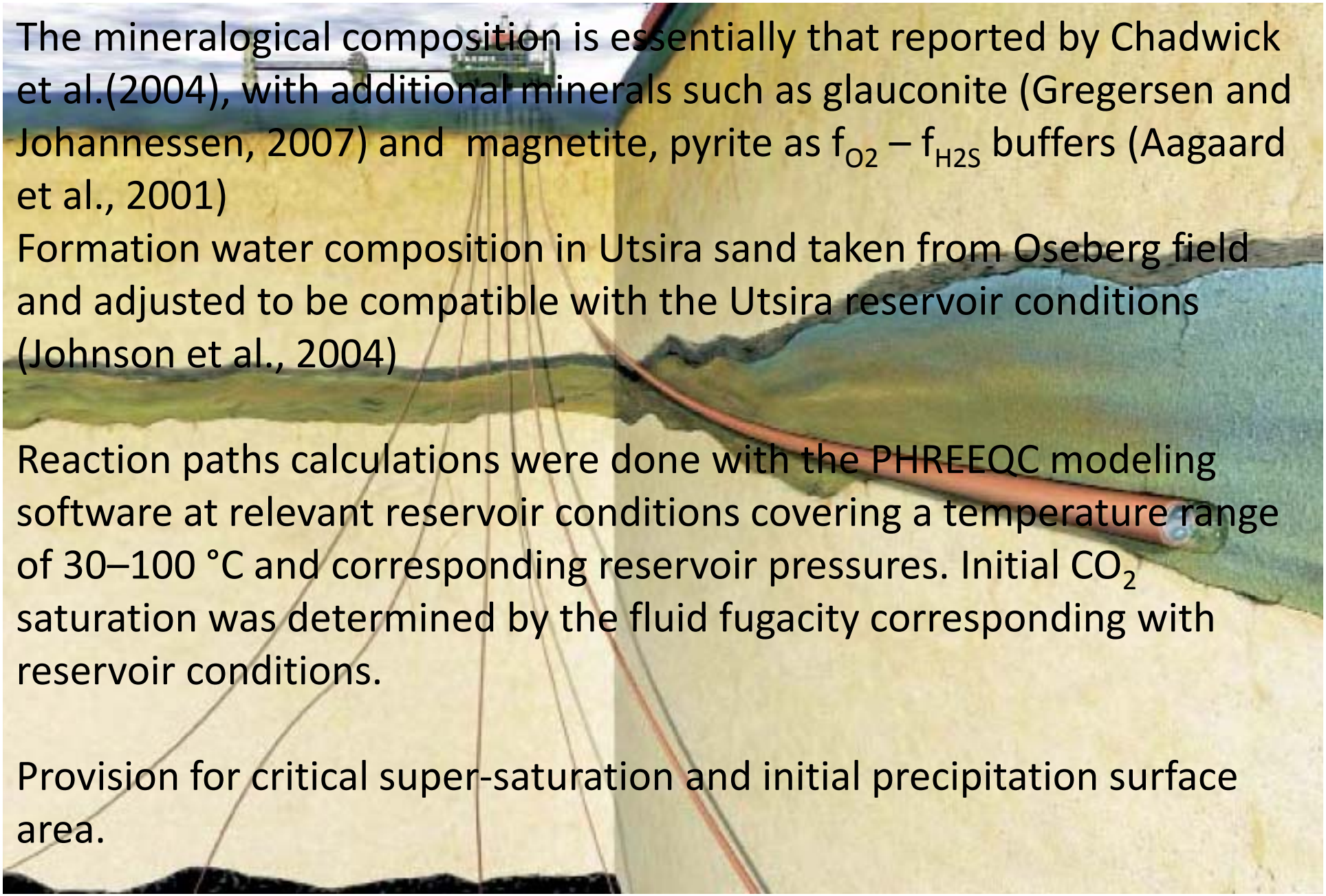

The mineralogical composition is essentially that reported by Chadwick et al.(2004), with additional minerals such as glauconite (Gregersen and Johannessen, 2007) and magnetite, pyrite as $f_{O2} – f_{H2S}$ buffers (Aagaard et al., 2001)

Formation water composition in Utsira sand taken from Oseberg field and adjusted to be compatible with the Utsira reservoir conditions (Johnson et al., 2004)

Reaction paths calculations were done with the PHREEQC modeling software at relevant reservoir conditions covering a temperature range of 30–100 °C and corresponding reservoir pressures. Initial CO_2 saturation was determined by the fluid fugacity corresponding with reservoir conditions.

Provision for critical super-saturation and initial precipitation surface area.

Redox conditions following the approach of Helgeson & Shock

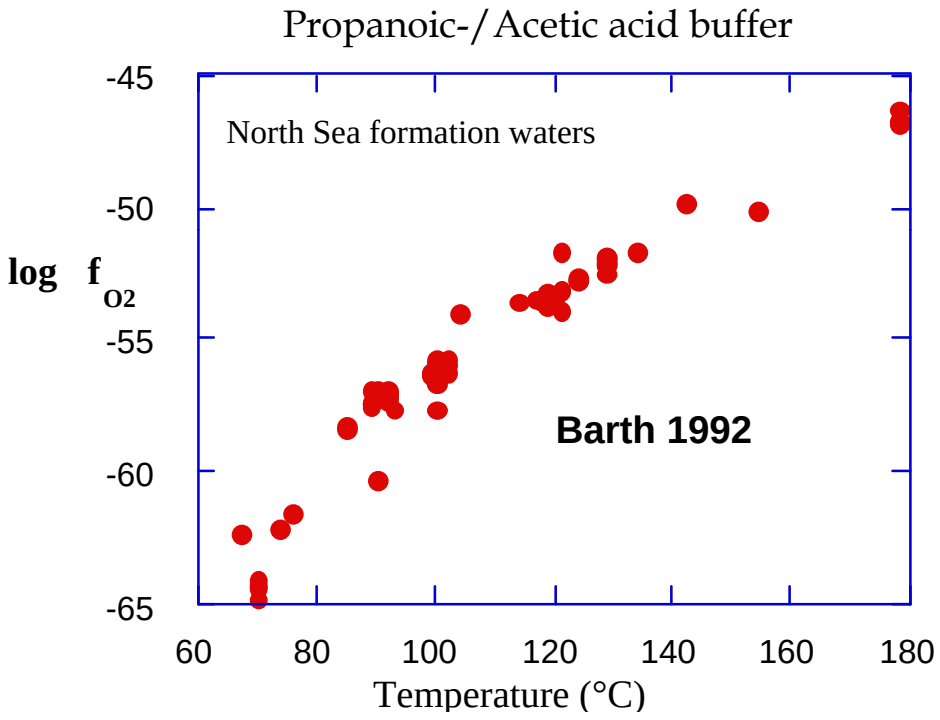

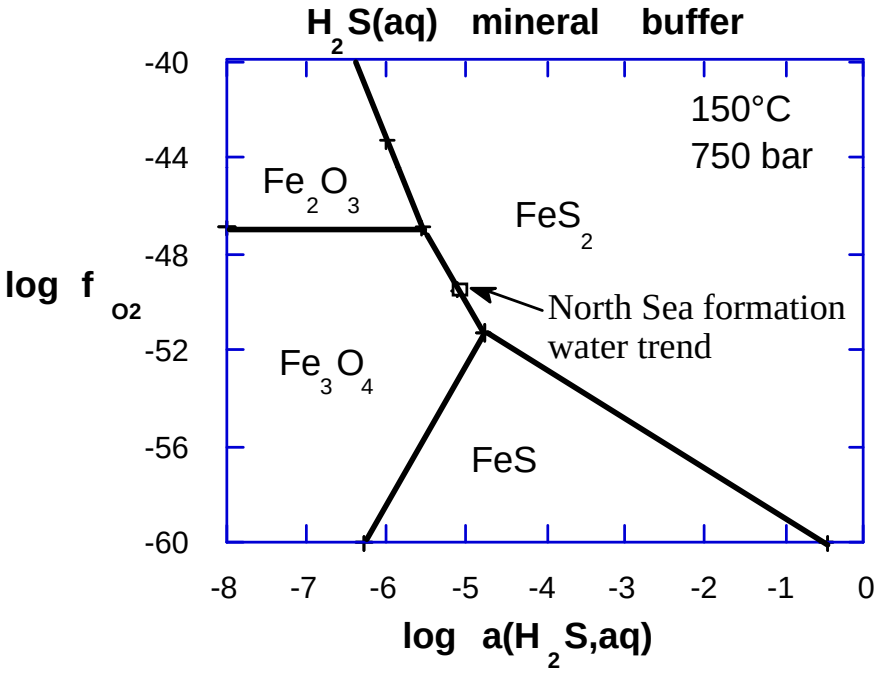

Utsira mineralogy

Mineral fractions included in the model (Chadwick et al., 2004). Total amount of clay minerals is assumed to be 4% for the base case.

Mineral	Weight%				
Primary	Base case	0% glauconite	2% glauconite	1% smectite	2% smectite
Quartz	72.5	73.5	71.5	72.5	71.1
Chalcedony	0	0	0	0	0
Albite	3.0	3.0	3.0	3.0	3.0
K-feldspar	13.0	13.0	13.0	13.0	13.0
Glauconite D	**1.0**	**0.0**	**2.0**	1.0	1.0
Clinochlore-14A	0.4	0.4	0.4	0.4	0.4
Smectite-high-Fe-Mg	0.6	0.6	0.6	**1.0**	**2.0**
Kaolinite	1.0	1.0	1.0	1.0	1.0
Muscovite	2.0	2.0	2.0	2.0	2.0
Magnetite	0.1	0.1	0.1	0.1	0.1
Pyrite	0.4	0.4	0.4	0.4	0.4
Calcite	6.0	6.0	6.0	6.0	6.0
Secondary					
Ankerite	0	0	0	0	0
Siderite	0	0	0	0	0
Dolomite	0	0	0	0	0
Magnesite	0	0	0	0	0
Dawsonite	0	0	0	0	0

Kinetic parameters used for rate calculations

Mineral	[a] $k_d^{37°C}$ (mol/m^2s)	[a] $k_p^{37°C}$ (mol/m^2s)	[b] α (m^2)	β BET (m^2/g)	[c] Ω_c	References
Quartz	4.08×10^{-14}	4.08×10^{-14}	1		100	Tester et al., (1994)
Albite	2.88×10^{-12}	2.88×10^{-12}	1	0.1	1	Brantley (2008)
K-feldspar	5.11×10^{-13}	5.11×10^{-13}	1	0.11	1	Brantley (2008) Gautier et al., (1994)
Glauconite	4.788×10^{-10}	4.788×10^{-10}	1	0.0178	1	Tardy et al.,(1994) Aagaard et al.,(2004)
Clinochlore-14A	2.8×10^{-12}	2.8×10^{-12}	1	1.6	1	Brandt et al., (2003) Nagy (1995)
Smectite-h-Fe-Mg	5.59×10^{-14}	5.59×10^{-14}	1	50	1	Amram and Ganor (2005) Golubev at al.,(2006)
Kaolinite	1.85×10^{-13}	9.21×10^{-15}	1		1	Yang and Steefel (2008)
Muscovite	7.63×10^{-14}	7.63×10^{-14}	1	0.68	1	Oelkers et al., (2008)
Magnetite	2.398×10^{-9}	2.398×10^{-9}	1	0.102	1	White et al.,(1994)
Pyrite	2.62×10^{-9}	2.62×10^{-9}	1	0.051	1	Williamson and Rimstidt (1994)
Calcite	Equilibrium	Equilibrium	-	-	-	

Kinetic parameters used for precipitation rate calculations

Mineral	$^{a}k_d^{37°C}$ (mol/m^2s)	$^{a}k_p^{37°C}$ (mol/m^2s)	$^{b}\alpha$ (m^2)	β BET (m^2/g)	$^{c}\Omega_c$	References
Chalcedony	4.08×10^{-14}	4.08×10^{-14}	0.1 – 100	0.0225	1	Tester et al., (1994)
Calcite	Equilibrium	Equilibrium	-	-	-	
Ankerite	1.27×10^{-7}	$1.27 \times 10^{-9 \pm 2}$	0.1 – 100	0.016	1 - 10	As dolomite
Siderite	2.76×10^{-7}	$2.76 \times 10^{-9 \pm 2}$	0.1 - 100	0.175	1 - 10	Golubev et al., (2009)
Magnesite	9.04×10^{-10}	$1.96 \times 10^{-14 \pm 2}$	0.1 - 100	0.127	1 - 10	Pokrovsky et al., (2009) Saldi et al.,(2009)
Dolomite	1.27×10^{-7}	$6.03 \times 10^{-9 \pm 2}$	0.1 - 100	0.016	1 - 10	Pokrovsky et al., (2005; 2009) Arvidson & Mackenzie(1997)
Dawsonite	4.85×10^{-9}	$4.85 \times 10^{-13 \pm 2}$	0.1 - 100	9.8	1 - 10	Declercq et al. (2009)

Utsira case revisited: mineralogical changes during storage

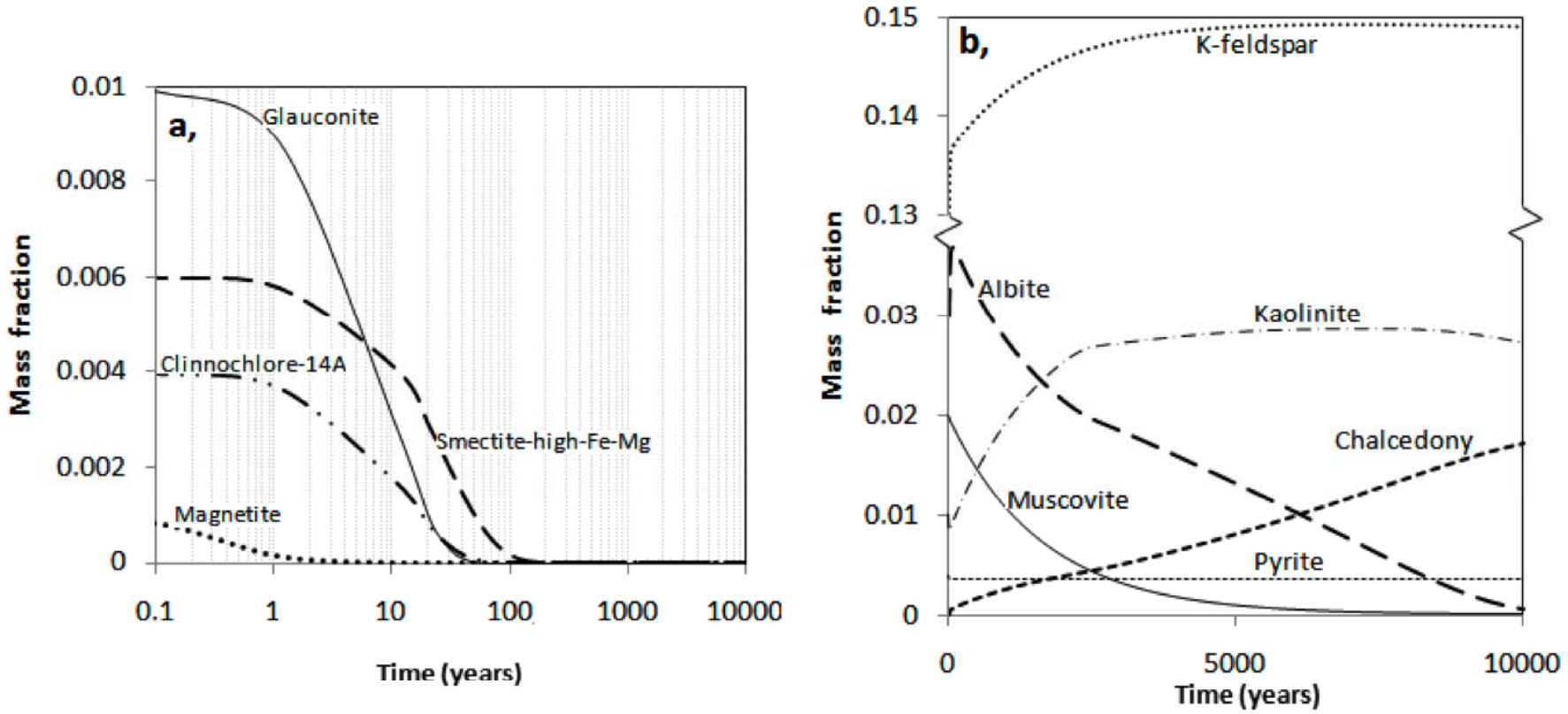

Changing mass fraction of minerals during interaction of the formation water and the sediments with CO_2 injected at 100 bars (base case). Note rapid dissolution of reactive clay minerals

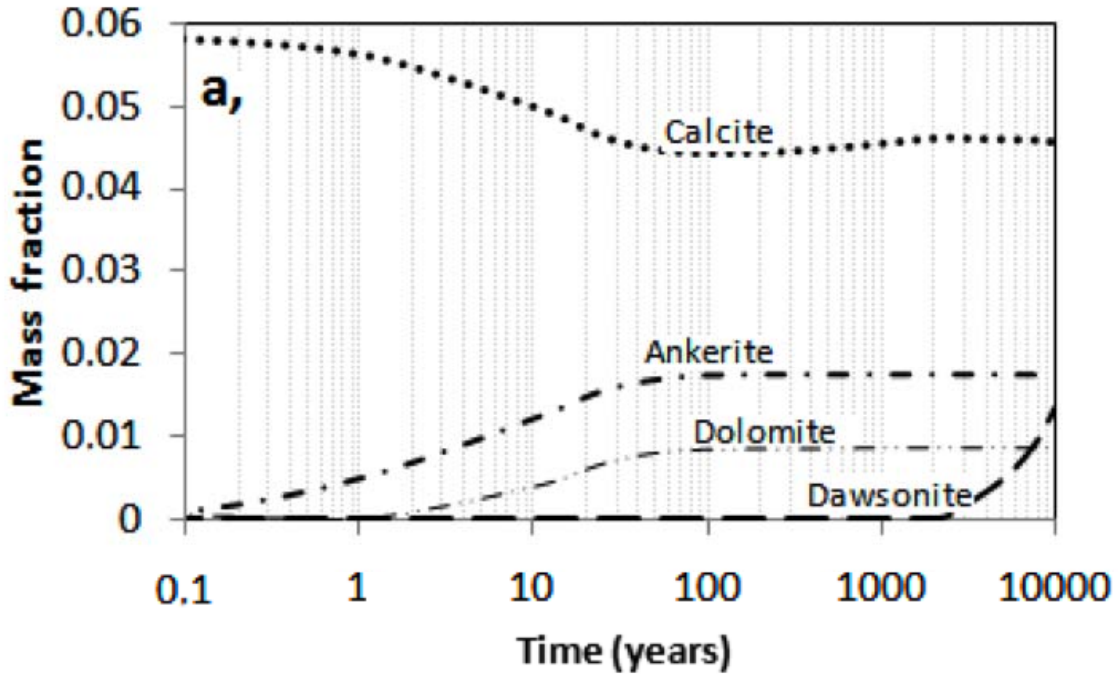

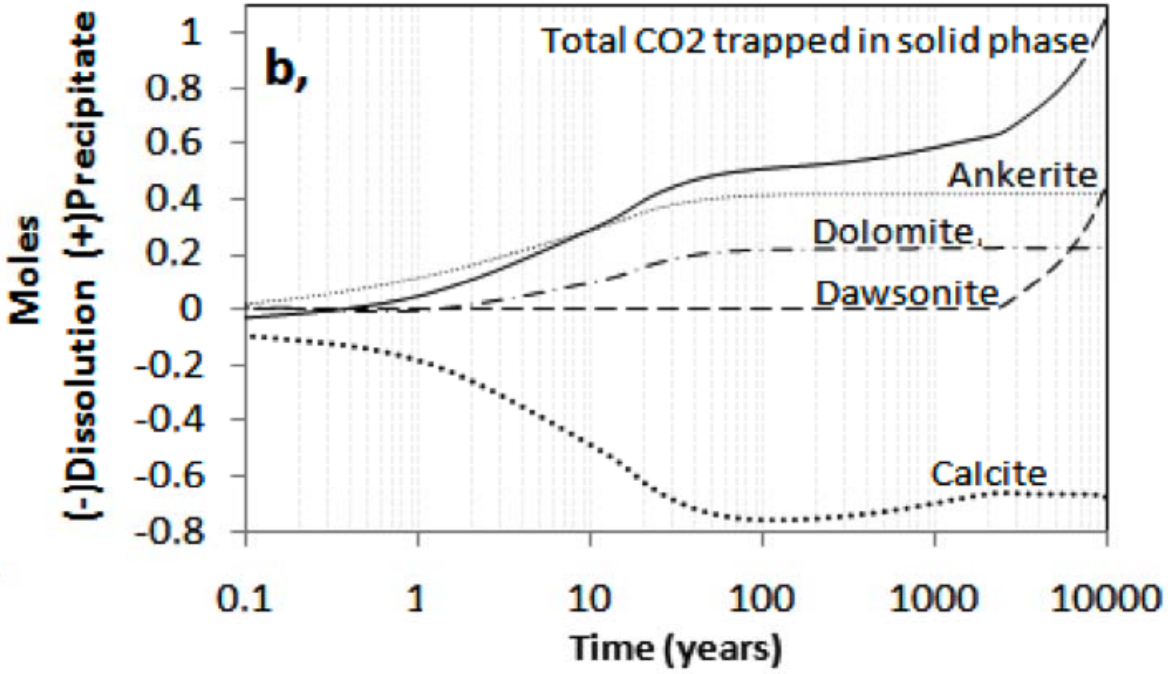

Utsira case revisited: carbonate reactions

Carbonate minerals and CO_2 trapped in solid phase in the base case where glauconite is 1%.

CO_2 is trapped in the three carbonate minerals ankerite, dolomite and dawsonite during 10 000 years of CO_2 sequestation

Utsira case revisited: Porosity changes due to mineral reactions

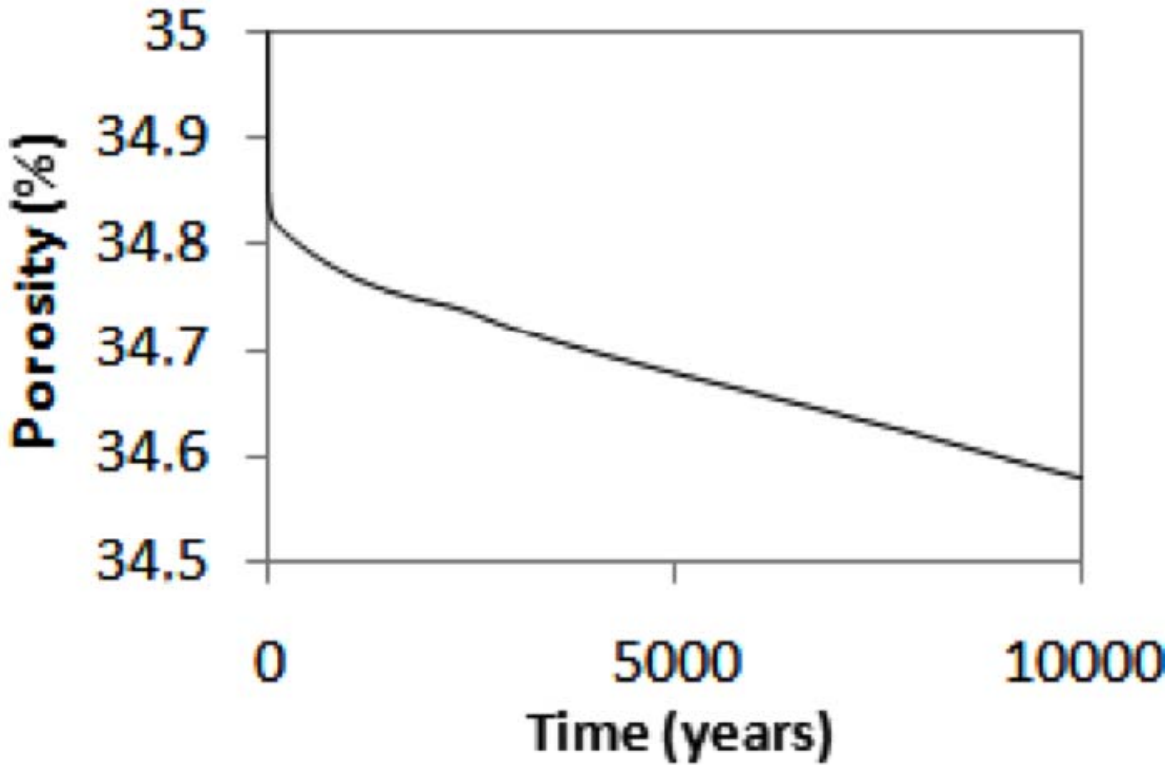

Porosity reduction during 10 000 years of CO_2 storage (base case)

Sensitivity of carbonate formation on the abundance of clays

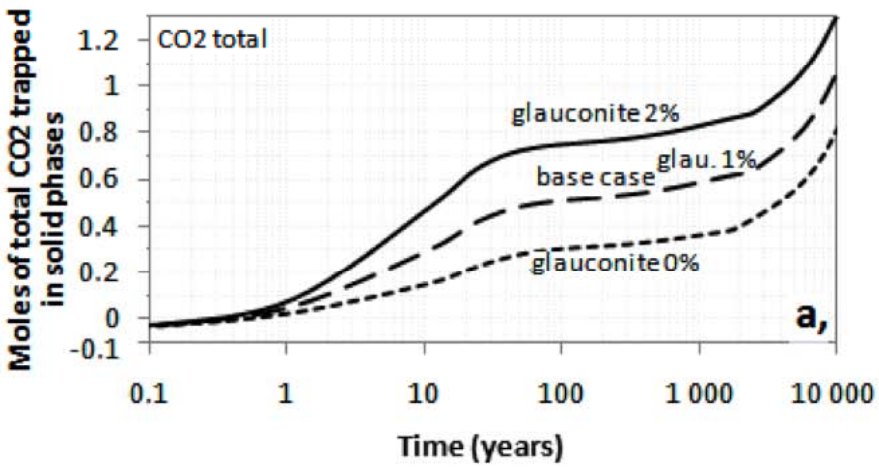

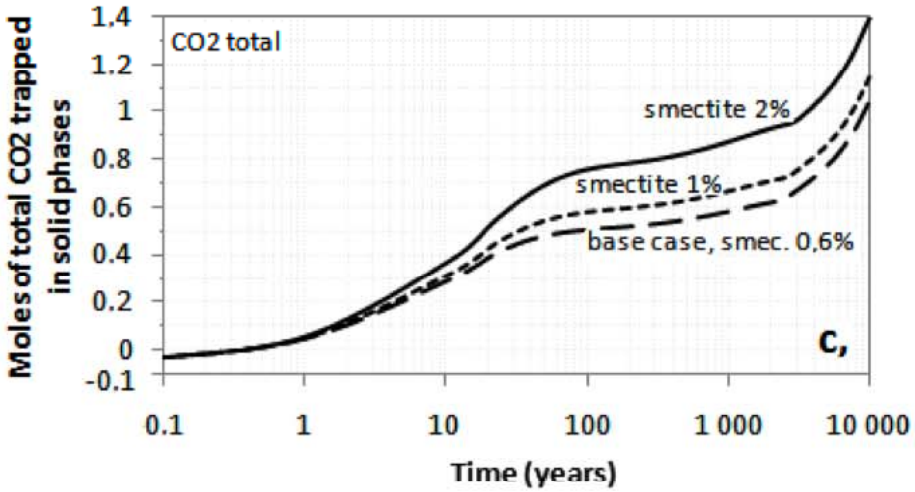

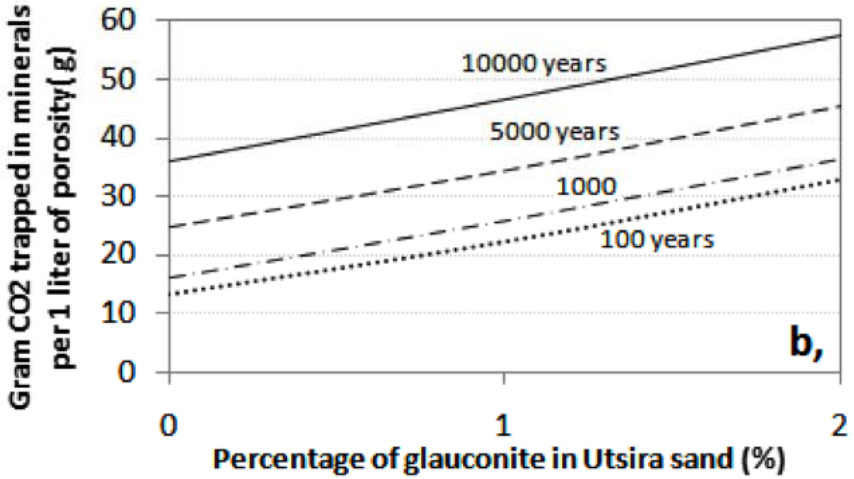

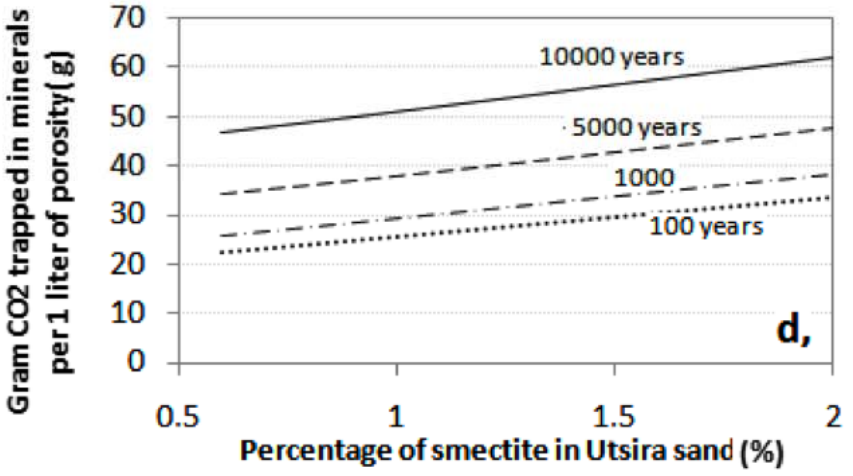

Total CO_2 trapped in carbonate minerals is proportional to the amount of glauconite and smectite. The smectite-dissolution reaction is slightly slower than glauconite at 37 ^{o}C

Sensitivity of carbonate formation on α

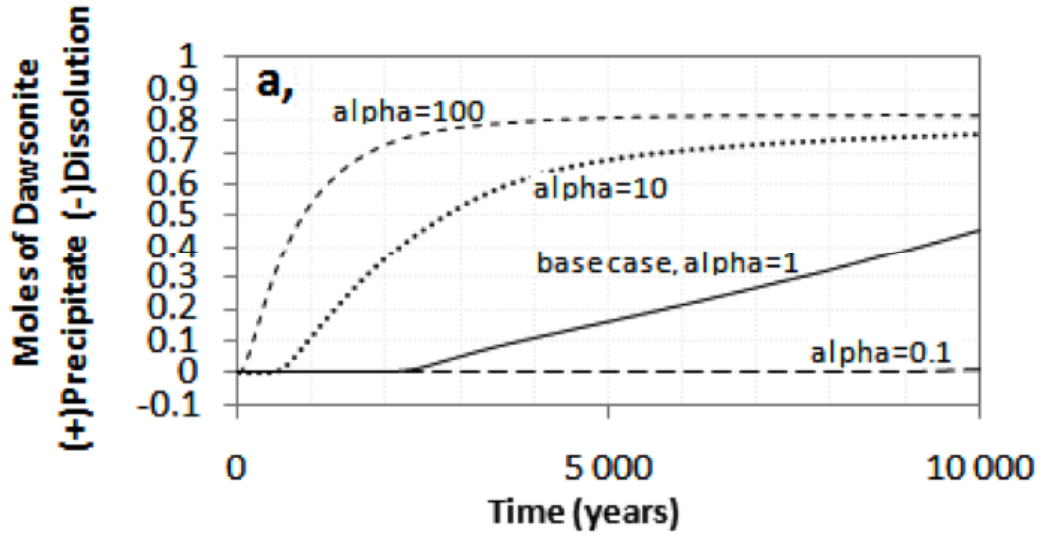

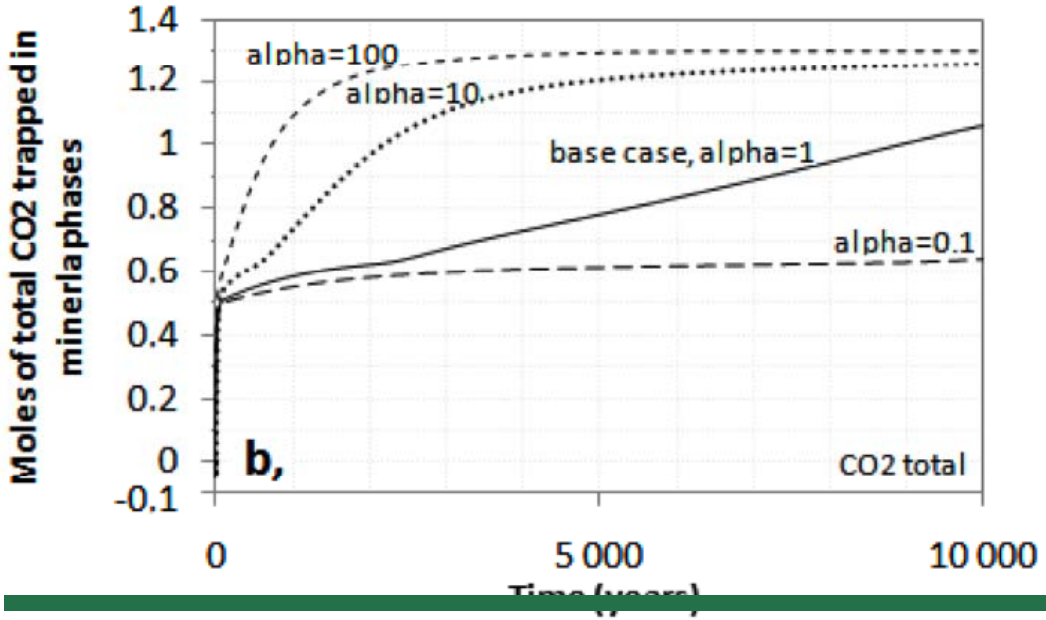

Moles of CO_2 trapped in carbonate minerals changes accordingly with moles of dawsonite precipitating that in turn is partly dependent on α.

The amounts of ankerite and dolomite remains rather constant.

Effect of $\alpha_{(Dawsonite)}$ on other mineral reactions

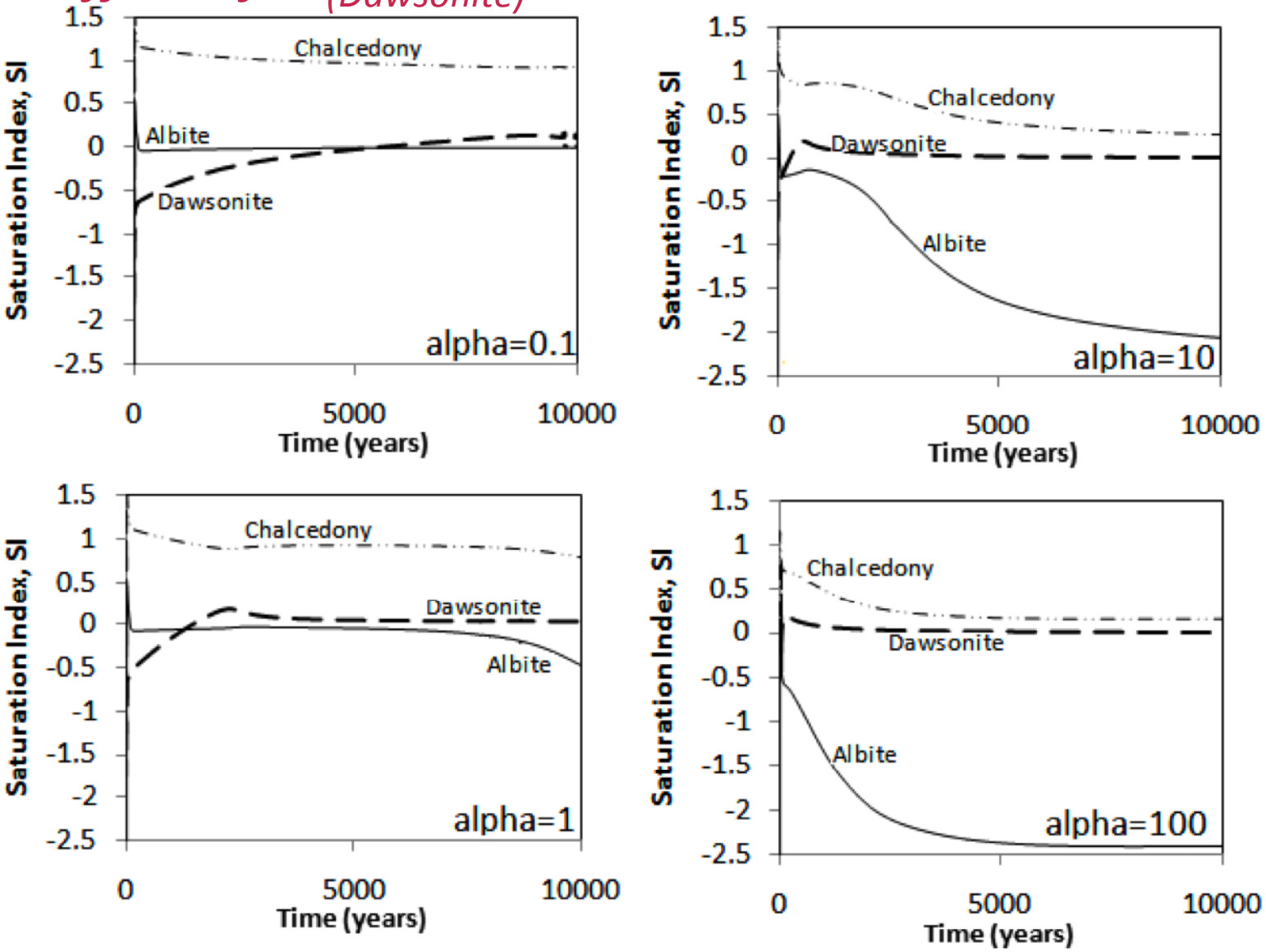

Saturation index of albite, chalcedony, dawsonite

Effect of α (Dawsonite) on albite reactions

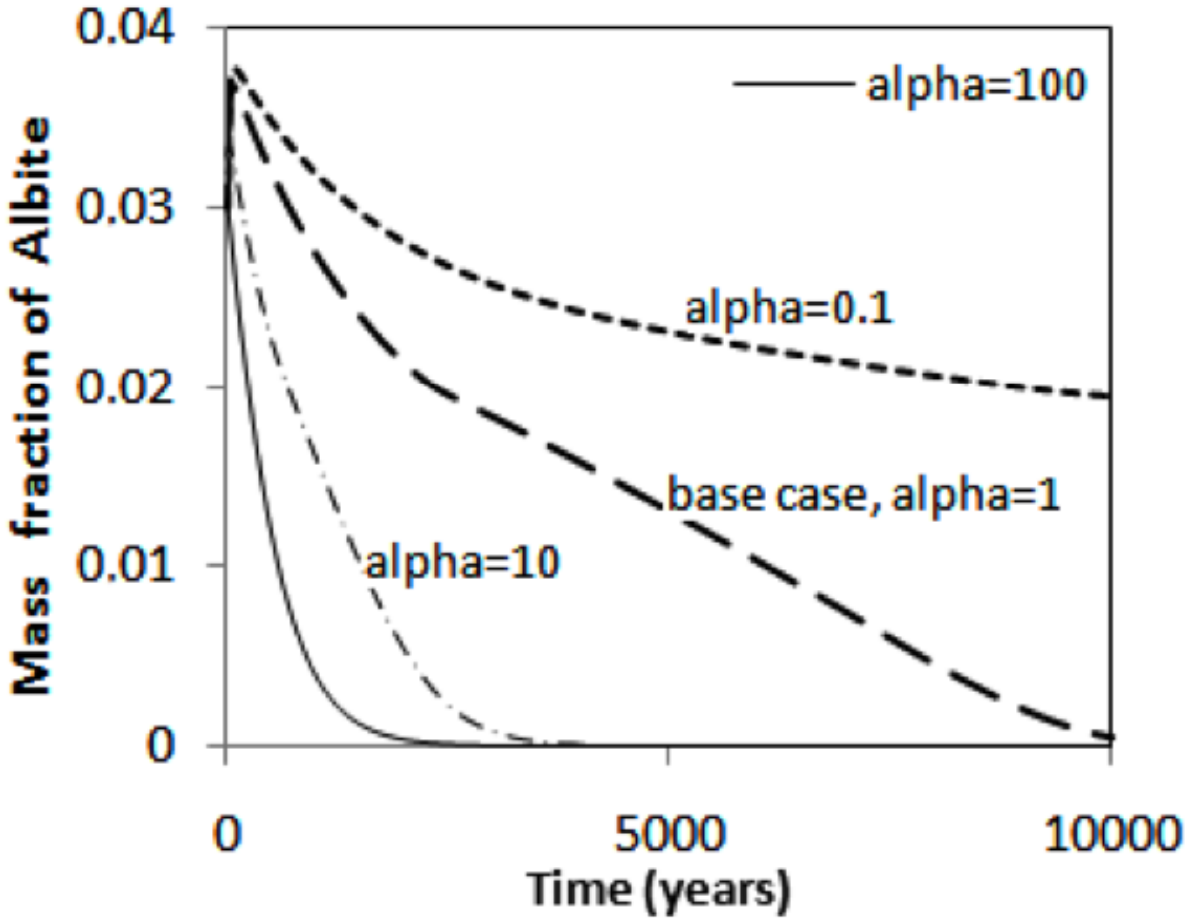

Mass fraction of albite

Sensitivity of carbonate formation on Ω_c

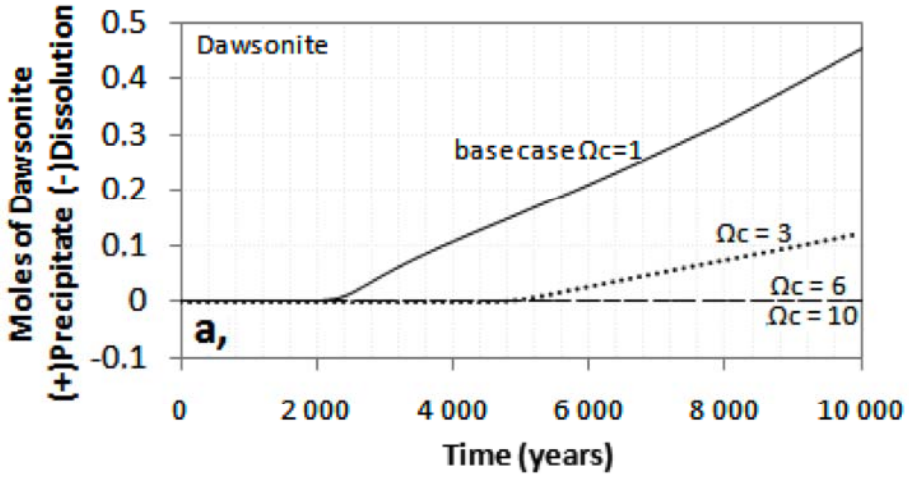

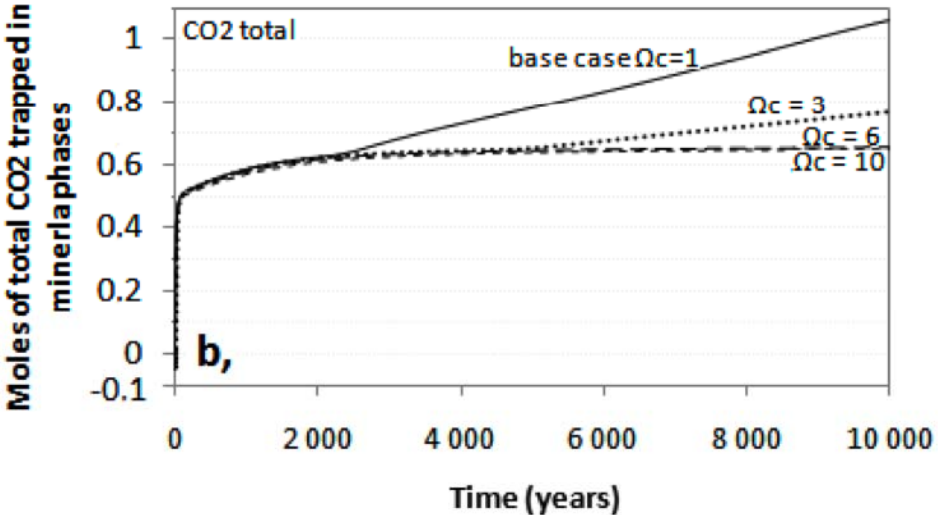

Moles of CO_2 trapped in carbonate minerals changes accordingly with moles of dawsonite precipitating that in turn is dependent on Ωc.

The amounts of ankerite and dolomite remains rather constant.

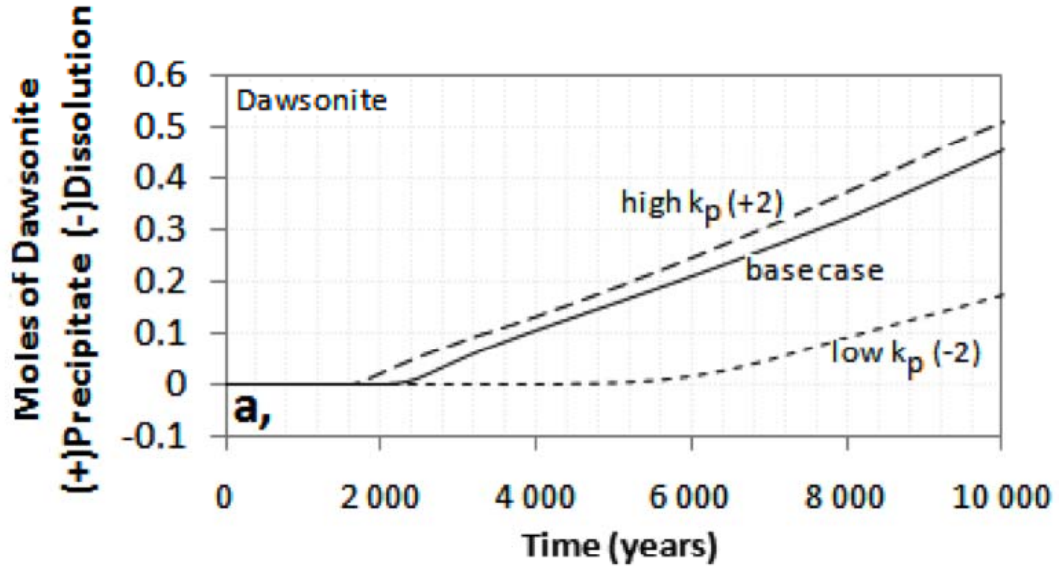

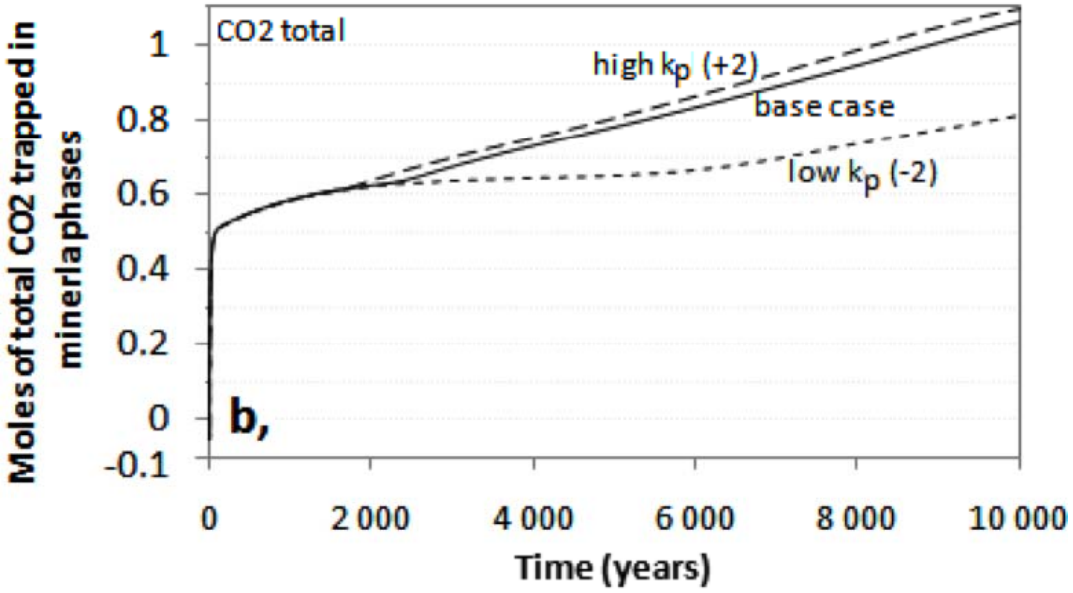

Sensitivity of carbonate formation to the precipitation rate coefficients, k_p.

Moles of CO_2 trapped in carbonate minerals changes accordingly with moles of dawsonite precipitating that in turn is dependent on k_p.

The amount of ankerite and dolomite remained almost constant after 10 000 years of CO_2 storage

Summary

The classical way of simulating mineral growth in CO_2 charged reservoirs by using a single-affinity-term TST-derived rate law fails to capture the difference in rate properties between under- and supersaturated systems

The Utsira case simulations were run over a period of 10000 years.

The main simulation results included dissolution of glauconite, smectite, chlorite, muscovite and albite, with precipitation of the carbonates siderite, ankerite, and minor dawsonite, as well as kaolinite, silica (either chalcedony or quartz), and K-feldspar. Resulting porosity changes were minimal.

Ankerite and dolomite formed rather early as a function of reactive clay mineral dissolution, while the formation of dawsonite was restricted to considerable longer reaction time.

The uncertainties in the simulations are specially connected with initial mineral abundances, specially clay minerals.